Tactile Sensing Using Tensor Cell

Hiroyuki SHINODA, Naoki MORIMOTO and Shigeru ANDO
Department of Mathematical Engineering and Information Physics
Faculty of Engineering, The University of Tokyo
7-3-1 Hongo, Bunkyo-ku, Tokyo 113, Japan

Abstract

In this paper, we propose a new tactile sensory structure using integrated sensing elements what we call "tensor cell". It is located sparsely in a flexible body of tactile sensor, and samples there the complete information of stress tensor which requires six degrees of freedom to describe it. We clarify first the advantage of this architecture theoretically based on the elasticity theory and the matrix algebra. Then the design of the actual tensor cell and experimental results are described, and an application of it to contact surface characterization is shown.

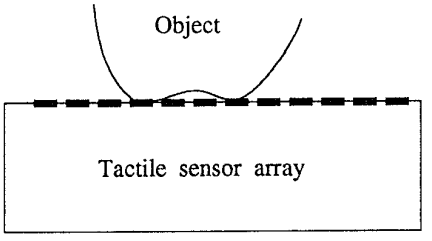

(a) Usual uniform array

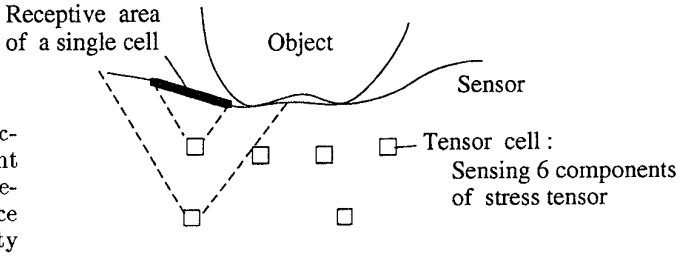

(b) Our array

Fig. 1 Schematic diagram of the tensor cell tactile sensor.

1 Introduction

In this paper we describe a new architecture of tactile sensor based on a complete stress sensing element "Tensor Cell." Among the previous works, some researchers proposed a sensor array to detect surface three stress components, and pointed out the necessity of sheer stress detection[1, 2]. De Rossi, et al., emphasized the importance of stress-component discrimination in the sensor body based on the observation of human skin[3], and attempted to solve an inversion problem of surface fine stress distribution[4, 5, 6].

In this paper, we emphasize the role of elastic body with sparse tensor cells for direct perception of surface tactile features, as it is suitable for protecting the sensing elements from mechanical damage and giving softness of the tactile sensor.

The goal of us is to develop a tactile sensor which obtain various useful tactile information by simple signal processing and simple fabrication of the sensor using three-dimensional structure with inherent intelligence which resides in the physical property of elastic body [8, 9, 10].

The architecture and the most fundamental theory of the sensor will be presented. Then experimental results by scale-up model of tensor cell will be shown.

2 The Architecture and Its Advantages

Schematic diagram of our sensor is shown in Fig. 1. Comparing this structure with that of an usual 2-D array sensor (Fig. 1), we will be able to summarize the advantages as

1. Feature extraction capability of each element : As is described later, the eigen structure of stress tensor inner the body has an explicit relation to the class of contact style on the surface, thus,

IEEE International Conference
on Robotics and Automation
0-7803-1965-6/95 $4.00 ©1995 IEEE

the early stage of feature extraction is done by the aid of ideally continuous physical property without enormous sampling.

2. Easiness of fabrication:
   As a result of that ability, only sparse location of elements is sufficient. Rigorous homogeneity of the sensitivity among neighbor cells is not requested. Efforts of signal processor are lessened.

3. Softness :
   Compliant sensor body by the sparse location of the elements.

4. Use of 3-D space:
   Multi-scale perception of the surface pressure distribution without any computation, which greatly improves the feature extraction ability from both still and dynamic pattern[8, 11].

Especially in the following description, we clarify the feature extraction capability which resides in a single tensor cell.

3 Stress Tensor vs. Contact Dimension

Before all of discussions, we confirm following matters.

1. Since the stress tensor matrix T submits to tensor transform, it can be completely characterized by three eigenvectors and eigenvalues of the tensor matrix. In this paper we graphically illustrate tensor by eigenvectors weighted by corresponding eigenvalue which overlap with the principal axes of stress ellipsoid.

2. Kernel of T is defined as a vector space spanned by eigenvectors of zero eigenvalue.

3.1 Stress tensor by a point force

Suppose there exists a point force $\mathbf{F}$ on the surface of half infinite elastic body(Fig. 2). Under the polar coordinate, the stress tensor is expressed as[12]

$$\begin{pmatrix} \sigma_{rr} & \sigma_{r\theta} & \sigma_{r\psi} \\ & \sigma_{\theta\theta} & \sigma_{\theta\psi} \\ * & & \sigma_{\psi\psi} \end{pmatrix} = \frac{3}{2\pi r^2} \begin{pmatrix} -F_r & 0 & 0 \\ & 0 & 0 \\ * & & 0 \end{pmatrix}$$

$$+ \frac{3}{2\pi r^2} \frac{1-2\sigma}{3} (A_1 F_r + A_2 F_\theta + A_3 F_\psi) \quad , \quad (1)$$

$$A_1 = \frac{1}{1+\cos\theta} \begin{pmatrix} \sin^2\theta & \sin\theta\cos\theta & 0 \\ & \cos^2\theta & 0 \\ * & & \cos\theta \end{pmatrix}, \quad (2)$$

$$A_2 = \frac{-\sin\theta}{(1+\cos\theta)^2} \begin{pmatrix} \sin^2\theta & \sin\theta\cos\theta & 0 \\ & \cos^2\theta & 0 \\ * & & -1 \end{pmatrix}, \quad (3)$$

$$A_3 = \frac{-\sin\theta}{(1+\cos\theta)^2} \begin{pmatrix} 0 & 0 & \sin\theta \\ & 0 & \cos\theta \\ * & & 0 \end{pmatrix}, \quad (4)$$

where $(F_r, F_\theta, F_\psi) \equiv \mathbf{F}$ expresses the point force by the polar coordinate. Regarding to typical dense and soft rubber-like material, the term $(1-2\sigma)/3$ is within order of 1% while any component of A_1,A_2, and A_3 is less than 1 where $\theta < \pi/2$. Therefore we will neglect the term of $(1-2\sigma)$ in following discussions.

Then we know that under a single point contact, the rank of the stress tensor is 1, and it has only one non-zero eigenvalue with an eigenvector parallel to the line passing through the contact point and observing point. The non-zero eigenvalue equals a contact force weighted by the cosine rule and an inverse squared distance from the contact point to the cell.

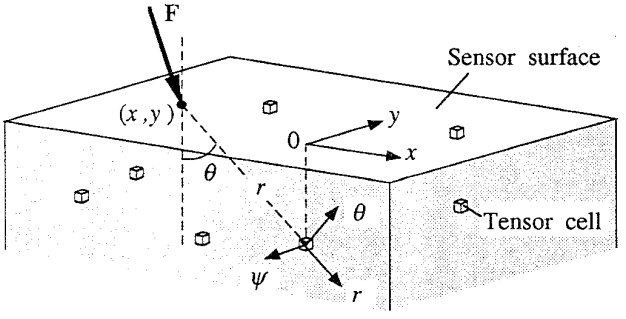

Fig. 2 Coordinate systems.

3.2 General case

If distributed surface forces $\mathbf{F}_i(x_i, y_i)$ are given, the internal stress tensor T is written as a sum of each stress tensor element t_i from each surface force element $\mathbf{F}_i$,

$$T = \sum_i t_i. \quad (5)$$

And each $t_i(\mathbf{F}_i)$ was given in the previous section.

3.3 Contact classification by rank

Now let us consider the eigen structure of tensor matrix T for various contact classes.

1. If the contact is concentrated to one point, the matrix T has only one non-zero eigenvector parallel to the line passing through the contact point and the observing point.

2. If the contact is concentrated on a line, each kernel of tensor t_i has a common basis which is orthogonal to the plane spanned by the line and observing point. Therefore, the rank of T cannot exceed 2, moreover except for a trivial case, it can be said that the rank of T equals 2, while the two non-zero eigenvectors are on that plane.

3. If the contact is spread, except for a trivial case, all the eigenvalues are non-zero.

We summarize this in Fig. 3 and Table 1. It is clarified that rank of the tensor corresponds to the dimension of the expansion of surface stress distribution, and concentrated distribution is localized by the direction of eigenvector.

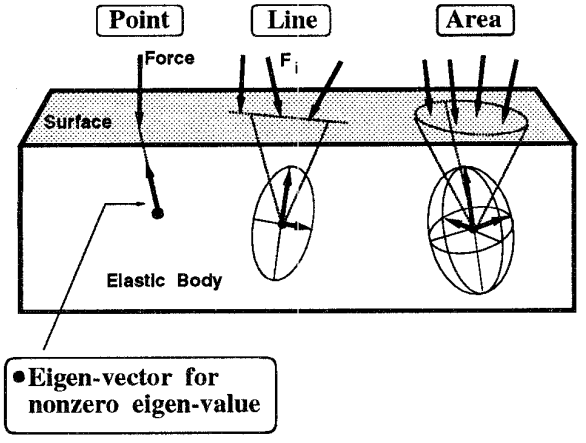

Fig. 3 Eigenvectors of stress tensor with stress ellipsoid for various contact.

Table 1 Contact style vs. eigen structure.

Contact style	Rank	Eigenspace
point	1	A line including contact point and cell
line	2	A plane including contact line and cell
Area	3	Entire space

3.4 Evaluating contact position and extent from stress element

Next we will explain another ability of tensor cell. From Eq.(1) and (5), stress tensor at $(0,0,-z_0)$ under distribution of $\mathbf{F}_i(x_i, y_i)$ is rewritten by Cartesian coordinate as,

$$\begin{pmatrix} \sigma_{xx} & \sigma_{xy} & \sigma_{xz} \\ & \sigma_{yy} & \sigma_{yz} \\ * & & \sigma_{zz} \end{pmatrix} = \sum_i \mathbf{F}_i \cdot \mathbf{w}(x_i, y_i) \begin{pmatrix} {x_i}^2 & x_i y_i & x_i z_0 \\ & {y_i}^2 & y_i z_0 \\ * & & {z_0}^2 \end{pmatrix}, \tag{6}$$

where

$$\mathbf{w}(x,y) \equiv \frac{3}{2\pi(x^2+y^2+{z_0}^2)^{\frac{5}{2}}} \begin{pmatrix} x \\ y \\ z_0 \end{pmatrix}.$$

Therefore each stress tensor component is equivalent to the moment of distribution $\mathbf{F}_i \cdot \mathbf{w}_i$ ($\mathbf{w}_i \equiv \mathbf{w}(x_i, y_i)$) in case $\mathbf{F}_i \cdot \mathbf{w}_i < 0\ \forall i$. This assumption is almost always valid in case of usual contact condition (Fig. 4).

1)Top-left 2×2 sub-matrix

$\begin{pmatrix} \sigma_{xx} & \sigma_{xy} \\ \sigma_{xy} & \sigma_{yy} \end{pmatrix}$ → Second moment of $\mathbf{F}_i \cdot \mathbf{w}_i$.

2)Top 2 components of the right column

$(\sigma_{xz}, \sigma_{yz})$→ First moment.

3)The bottom-right

σ_{zz}→ Integral of the distribution.

It must be emphasized that such moments of surface force distribution are obtained only by one point of stress tensor.

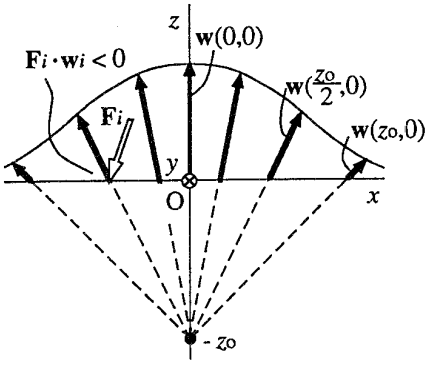

Fig. 4 Illustration of $\mathbf{w}(x,y)$.

Finally we write the equations which combine the stress tensor at $(0,0,-z_0)$ with parameters characterizing the spread of $\mathbf{F}_i \cdot \mathbf{w}_i$.

Center of distribution $\mathbf{F}_i \cdot \mathbf{w}_i$:

$$(x_G, y_G) = \frac{z_0}{\sigma_{zz}}(\sigma_{xz}, \sigma_{yz}), \tag{7}$$

Variance matrix:

$$\mathcal{M} = \frac{{z_0}^2}{\sigma_{zz}} \begin{pmatrix} \sigma_{xx} & \sigma_{xy} \\ \sigma_{xy} & \sigma_{yy} \end{pmatrix} - \begin{pmatrix} {x_G}^2 & x_G y_G \\ x_G y_G & y_G y_G \end{pmatrix}. \tag{8}$$

4 Realization of Tensor Cell

In this section, we realize an sized-up model of the tensor cell in order to validate the theory and usefulness of the architecture.

4.1 A design of cubic tensor cell

The conditions requested to the tensor cell will be enumerated as:

1. Homogeneous sensitivity to six stress components and discrimination capability.

2. Symmetric structure.

3. Compactness for the least disturbance to the neighbors.

In this paper, we attempted a cubic design of the tensor cell shown in Fig. 5.

On the three sides of a 6 mm by 6 mm rigid cube, chemical etched PVDF films were pasted.

The output voltage of the PVDF element only reflects the normal stress on it.

And six outputs as

1. Sum signals:
   $p_x = o_1 + o_2$, $p_y = o_3 + o_4$, $p_z = o_5 + o_6$

2. Differential signals:
   $q_{xy} = o_3 - o_4$, $q_{yz} = o_5 - o_6$, $q_{zx} = o_1 - o_2$

were detected where $o_i (i = 1, \cdots 6)$ is each output from each element i in Fig. 5.

From the symmetry, the outputs in a uniform stress field σ_{ij} are written as

$$\begin{pmatrix} p_x \\ p_y \\ p_z \end{pmatrix} = A \begin{pmatrix} 1 & -\alpha & -\alpha \\ -\alpha & 1 & -\alpha \\ -\alpha & -\alpha & 1 \end{pmatrix} \begin{pmatrix} \sigma_{xx} \\ \sigma_{yy} \\ \sigma_{zz} \end{pmatrix},$$
$$\begin{pmatrix} q_{xy} \\ q_{yz} \\ q_{zx} \end{pmatrix} = A\beta \begin{pmatrix} \sigma_{xy} \\ \sigma_{yz} \\ \sigma_{zx} \end{pmatrix}, \quad (9)$$

where α and β depend only on the Poisson's ratio σ and sensitive area of the etched PVDF. Regarding to our sensor, those parameters was obtained as α=0.24, β =0.36 by numerical calculation. In this case, any of the eigenvalues of the matrix in the upper equation equals 0.93, which means that any stress tensor component can be obtained stably. The disturbance to the surrounding stress field decreases in proportion to inverse cubed distance from the cell, thus, the depth and interval of cell location should be several times larger than the cell size.

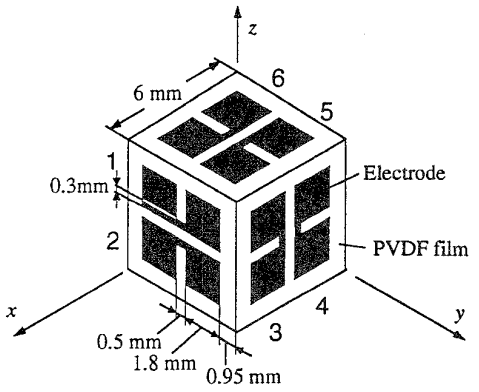

(a)

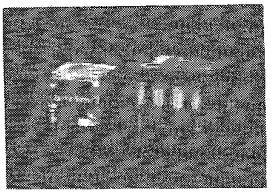

(b)

Figure 5: (a) Structure of the tensor cell. PVDF films with patterned electrodes are placed on a rigid cube. (b) Photograph of the tensor cell.

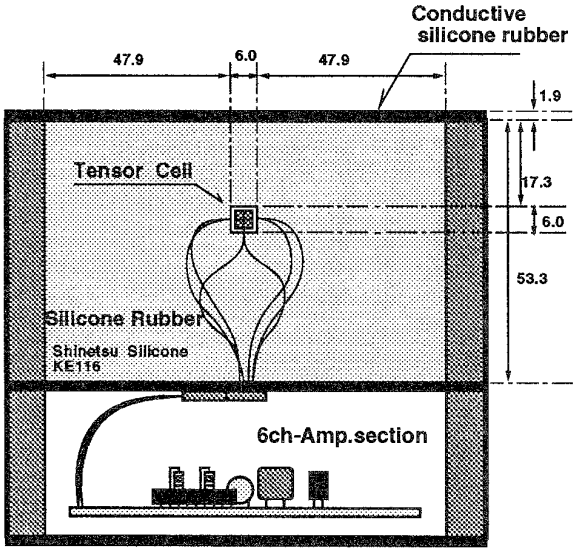

Fig. 6 Experimental set-up. A tensor cell in silicone rubber with 6 channel charge amplifier.

5 Experiments

The fabricated cell was located inside of silicone rubber 19 mm below the surface as illustrated in Fig. 6. The output was obtained through 6 channel charge amplifier, and electrical shield was brought by the surface conductive rubber. In Fig. 7(a), sensor outputs under a single point contact (vertical indentation of a sphere with radius 5mm, maximum force 0.8 [N]) at $(x, y) = (1,0)$[cm] is shown. And Fig. 7(b) shows its stress ellipsoid at $t = 0.21$ sec. It is seen that the maximum eigenvalue is sufficiently larger than the second and the third eigenvalue, and the major eigenvector points at the contact position.

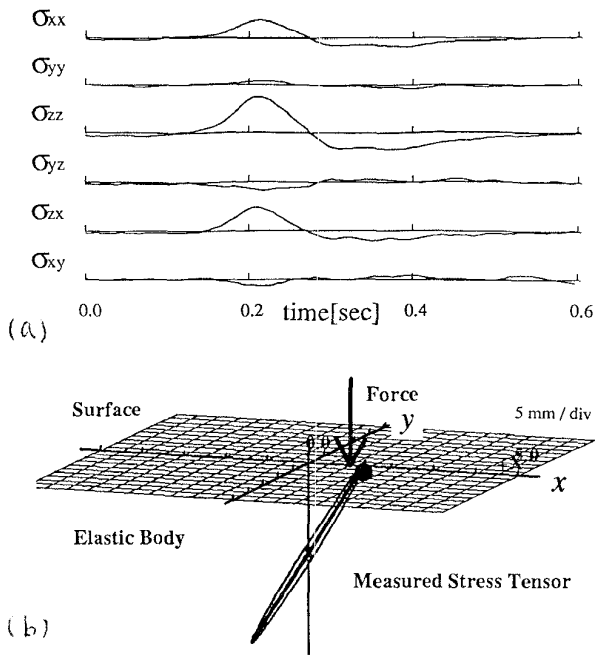

Fig. 7 (a) Outputs of the tensor cell given a point force at $(x, y) = (1,0)$ [cm]. (b) Stress ellipsoid at the peak (t= 0.21 sec).

Fig. 8 shows the detected positions by tensor cell under some single point contacts at various positions. The tensor cell could detect contact positions $1 \sim 2$ mm accuracy from the directions of major eigenvectors. For all of the data, the ratios of second eigenvalue to maximum eigenvalue were less than 10%.

Fig. 9 and 10 shows the stress ellipsoids from the tensor cell under the contact by a line edge along $x = 0$, and cylinder 40 mm in diameter respectively. In Fig. 9, the maximum and the second eigenvalues were sufficiently larger than the third which means it was detected that the distribution of the surface stress was concentrated on a line. And the two major eigenvectors spanned a plane including the contact line. In Fig.10 all eigenvalues were in comparable order.

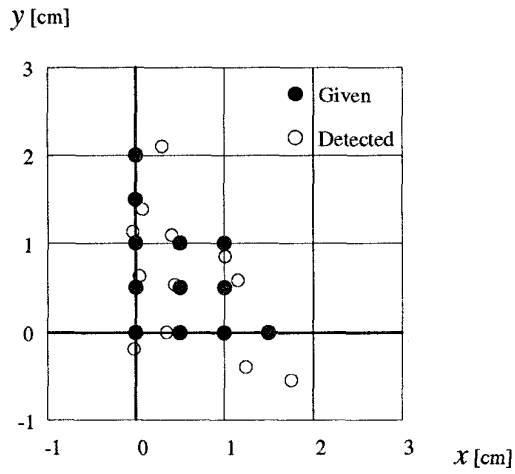

Fig. 8 Results of point-contact localization by the directions of major eigenvectors.

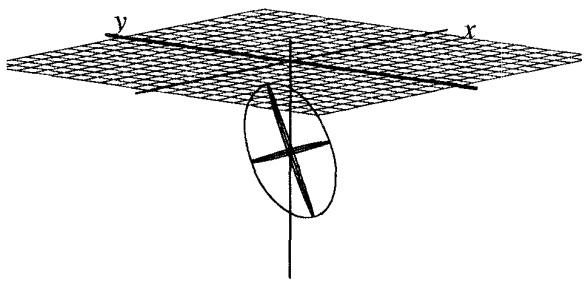

Fig. 9 Stress ellipsoid for a line edge along y axis.

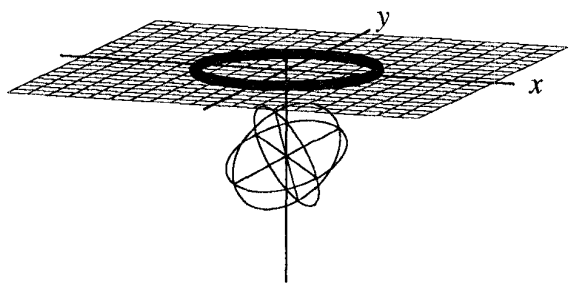

Fig. 10 Stress ellipsoid for a spread object (a cylinder 40 mm in diameter).

Fig. 11 shows the results of quantitative evaluation of contact spread under vertical indentation. The indented objects were a line edge along $x = 0$, a cylinder 30 mm in diameter and a ring whose inside and outside diameter were 35 mm and 50 mm, respectively. The ellipses in the figure were drawn so that the center overlaps with (x_G, y_G) of Eq.(7), and major and minor axis are parallel to eigenvectors of $\mathcal{M}$ of Eq.(8), and equal to square root of the larger and smaller eigenvalue of it, respectively.

It was displayed that even a single tensor cell can perceive several important features of the contact style on the surface.

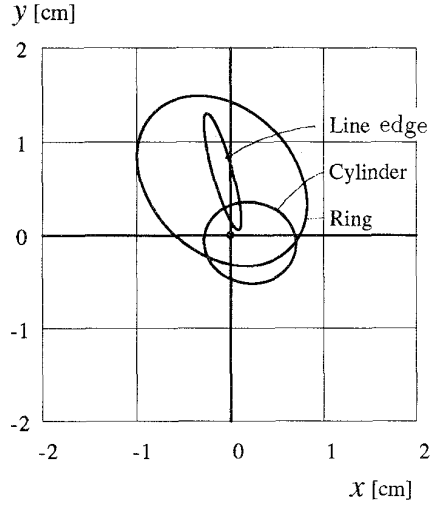

Fig. 11 Sensing of the spread of contact by Eq.(7) and (8), for vertically indented objects.

6 Conclusion

1. We proposed a tactile sensory architecture based on "tensor cell," an unit to detect all components of stress tensor in an elastic body.

2. Theoretically we clarified that the rank of inner stress tensor matrix corresponds to the dimension of the spread of contact, and the spread and position can be evaluated by the stress tensor directly.

3. An experimental scale-up model of 6 mm by 6 mm tensor cell was located in silicone rubber 19 mm below the surface, and

   (a) Correspondence between the rank of the stress tensor and spread of contact was examined for three kinds of objects : a small sphere with radius 5 mm, a line edge and a cylinder 40 mm in diameter.

   (b) Point contact was localized from the major eigenvectors of the stress tensor with accuracy of $1 \sim 2$ mm.

   (c) Two-dimensional spreads and positions of contact were quantitatively evaluated for vertically indented objects : a line edge, a cylinder and a ring.

References

[1] S. Hackwood, B. Beni, L. A. Hornak, R. Wolfe and T. J. Nelson, "A Torque Sensitive Tactile Array for Robotics," Int. J. Robotics Res, Vol.2, No.2, pp.46-61, 1983.

[2] H. C. J. M. Van Gestel, A. Bossche and J.R. Mollinger, "On-Chip Piezoresistive Stress Measurement in Three Directions," Sensors and Actuators A, Vol. 25, No. 27, pp.801-807, 1991.

[3] D. De Rossi, et al., "Biomimetic Tactile Sensor with Stress-Component Discrimination Capability," J. Molecular Electronics, Vol.3, pp.173-181, 1987.

[4] D. De Rossi, A. Caiti, R.Bianchi and G.Canepa, "Fine-Form Tactile Discrimination through Inversion of Data from a Skin-Like Sensor," Proc. 1991 IEEE int. Conf. on Robotics and Automation, pp.398-403, 1991.

[5] G. Canepa, M. Morabito, D. De Rossi, A. Caiti and T. Parisini, "Shape from Touch by a Neural Net," Proc. 1992 IEEE Int. Conf. on Robotics and Automation, pp.2075-2080.

[6] G. Canepa, M. Morabito and D. De Rossi, "Shape Estimation with Tactile Sensors : A Radial Basis Functions Approach," Proc. 31st IEEE Conf. on Decision and Control, pp.3493-3495, 1992.

[7] R. E. Ellis and M. Qin, "Singular-Value and Finite-Element Analysis of Tactile Shape Recognition," Proc. 1994 IEEE Int. Conf. on Robotics and Automation, Vol.3, pp.2529-2535, 1994.

[8] H. Shinoda and S. Ando, " A Tactile Sensing Algorithm based on Elastic Transfer Function of Surface Deformation," Proc. IEEE ICASSP'92, Vol.3, pp.589-592, San Francisco, 1992.

[9] H.Shinoda, M.Uehara and S.Ando, " A Tactile Sensor Using Three-Dimensional Structure," Proc. 1993 IEEE Int. Conf. Robotics and Automation, pp.435-441, Atlanta,1993.

[10] H. Shinoda and S. Ando, "Ultrasonic Emission Tactile Sensor for Contact Localization and Characterization," Proc. 1994 IEEE Int. Conf. Robotics and Automation, pp.2536-2543, 1994.

[11] S. G. Mallat, "Characterization of Signals from Multiscale Edges," IEEE Trans. on Pattern Analysys and Machine Intelligence, Vol. 14, No.7, pp.710-732, 1992.

[12] S.P.Timoshenko and J.N.Goodier: "Theory of Elasticity," McGraw Hill, 1970.